NJC

Accepted Manuscript

This is an *Accepted Manuscript*, which has been through the Royal Society of Chemistry peer review process and has been accepted for publication.

Accepted Manuscripts are published online shortly after acceptance, before technical editing, formatting and proof reading. Using this free service, authors can make their results available to the community, in citable form, before we publish the edited article. We will replace this *Accepted Manuscript* with the edited and formatted *Advance Article* as soon as it is available.

You can find more information about *Accepted Manuscripts* in the Information for Authors.

Please note that technical editing may introduce minor changes to the text and/or graphics, which may alter content. The journal's standard Terms & Conditions and the Ethical guidelines still apply. In no event shall the Royal Society of Chemistry be held responsible for any errors or omissions in this *Accepted Manuscript* or any consequences arising from the use of any information it contains.

ROYAL SOCIETY OF CHEMISTRY

www.rsc.org/njc

Synthesis and characterization of flower-like NiCoP/ZnO

Shuling Liu, Chenlu Ma

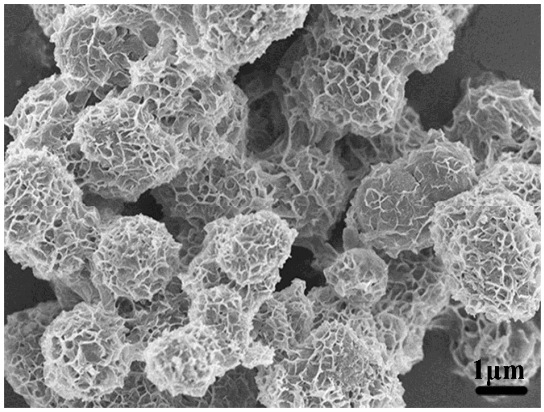

The ZnO nanosheets were successfully coated on the surface of NiCoP microstructure via solvothermal route.

Synthesis and characterization of flower-like NiCoP/ZnO

Shuling Liu[1,2*], Chenlu Ma[1,2]

[1]Key Laboratory of Auxiliary Chemistry & Technology for Chemical Industry, Ministry of Education, Shaanxi University of Science & Technology, Xi'an Shaanxi, 710021, PR China

[2]College of Chemistry & Chemical Engineering, Shaanxi University of Science & Technology, Xi'an Shaanxi, 710021, PR China

Abstract:

Flower-like NiCoP/ZnO composites were successfully synthesized via a simple solvothermal route. The as-prepared products were characterized by X-ray diffraction (XRD), energy dispersive X-ray spectrometer (EDS), scanning electron microscopy (SEM), and transmission electron microscopy (TEM). The materials characterization showed that the composites were composed of hexagonal NiCoP microspheres and hexagonal wurtzite ZnO nanosheets. And it could be observed that ZnO nanosheets with the wide 200-500nm and the thickness 50nm were assembled on the surface of NiCoP microspheres with the diameter of 1-2 μm. The BET surface area for the as-obtained samples calculated from the linear part of the BET plot are about 24.450 m^2 g^{-1} (NiCoP) and 88.412 m^2 g^{-1} (NiCoP/ZnO). Furthermore, it is also found that the NiCoP/ZnO composites exhibited superior adsorption performance for some organic dyes, such as Congo red and Malachite green, which may be related to the modification of ZnO nanosheets on the surfaces of NiCoP microspheres.

Keywords: Composites; Adsorption; NiCoP/ZnO.

1. Introduction

Bimetallic phosphides have attracted more and more attention to the researchers in recent years, because they show multiple functionalities and prominent catalytic activity, selectivity, and stability over monometallic phosphides. [1-4] Bimetallic phosphides are composed of two different metal atoms, which might produce a

* Corresponding author. Tel.: + 86-29-86168315; fax: 86-29-86168312. E-mail address: shulingliu@aliyun.com.

synergistic effect. The effect can further improve its properties. [5-8] However, it shows inferior adsorption performance for some typical organic dyes [9] , such as Malachite green, Congo red, etc. In order to solve the problem the authors intend to modified for the bimetallic phosphides.

Water pollution is one of the most serious problems at present. Semiconductor catalysts have been used to remove organic pollution in waste water. [10-12] It is well known that ZnO is an *n*-type semiconductor with a band gap of 3.2 eV and is an important multifunctional semiconductor with unique properties and many important applications. [13] Due to its low cost, nontoxicity, ZnO may be excellent adsorption material of organic dyes. The size, morphology and phase of products can determine performances for adsorption of some dyes. Thus, various synthesis methods have been employed to control particle morphology of ZnO, which can influence the properties. [14-18] Shang et al. successfully synthesized nano-plates, flower-like nanostructure of ZnO under hydrothermal condition. [19] Lu et al. reported the single-crystal ZnO nanowires using a vapor trapping chemical vapor deposition method. [20] Wei et al. had prepared graphene-ZnO hybrid via one-step electrochemical process and evaluated the photovoltaic performances. [21] Solvothermal method is chose in the paper because it exhibits many advantages such as mild preparation conditions, simplicity, low cost et al.[22] in the paper.

In this paper, NiCoP/ZnO composites were successfully fabricated by two-step solvothermal routes. The products were characterized using multiple techniques. And it is found that the composites were composed of hexagonal NiCoP microspheres and hexagonal wurtzite ZnO nanosheets, and ZnO nanosheets can be assembled uniformly on the surface of NiCoP microspheres. Further, compared to the NiCoP microspheres, the flower-like NiCoP/ZnO composites exhibited superior adsorption performance for some typical organic dyes, which may be applied in wastewater treatment.

2. Experimental

All of the chemical reagents were analytical pure grade and used without further purification.

2.1. Synthesis of the NiCoP microspheres

In a typical experimental procedure, an appropriate amount of $NiCl_2 \cdot 6H_2O$ (1mmol) and $CoCl_2 \cdot 6H_2O$ (2mmol) were dissolved in ethylene glycol under vigorously stirring into a Teflon-lined autoclave of 20 mL capacity at room temperature. After the mixture became homogeneous after stirring for 15 minutes, white phosphorus (3mmol) was added. The autoclave was sealed and maintained at 180℃ for 14 h. And then it was cooled to room temperature. The resulting black precipitate was filtered and washed successively with distilled water and absolute ethanol. Finally the as-obtained samples were dried in vacuum at 60℃ for 8 h and collected for characterization.

2.2. Synthesis of the flower-like NiCoP/ZnO composites

The as-prepared NiCoP precursor (2.7mmol) and $[Zn(CH_3COO)_2 \cdot 2H_2O]$ (0.9mmol) were dissolved in ethylene glycol under vigorously stirring into a Teflon-lined autoclave of 20 mL capacity at room temperature. After stirring 20 min, sodium hydroxide (0.5mmol) was added. The autoclave was sealed and maintained at 120℃ for 10 h. And then it was naturally cooled to room temperature. The resultant products were filtered and washed successively with distilled water and absolute alcohol for several times to remove the possible residues. Then the as-obtained samples were dried in vacuum at 60℃ for 8 h and collected for characterization.

2.3. Adsorption performance measurements

50 mg of the as-prepared (NiCoP and NiCoP/ZnO) were ultrasonic dispersed into 50 mL of dye solution with a concentration of 1×10^{-4}mol/L of Congo red and 1×10^{-5}mol/L Malachite green aqueous solutions. The as-obtained products were measured and analyzed at room temperature. The property changes of dyes (UV-Vis absorption spectra) were recorded on a Hach DR5000 ultraviolet-visible (UV-vis) absorption spectrophotometer in the wavelength ranging from 110 to 900 nm.

2.4. Characterization

X-ray diffraction (XRD) patterns of the as-prepared products were recorded using a Japan Rigalcu D/Max-3cx-ray diffractometer (Tokyo, Japan) with a Cu Ka radiation (λ=1.5418 Å). Field-emission scanning electron microscopy (FE-SEM) images were collected using a Japan Hitachi S-4800 FE-SEM (Ibaraki prefecture, Japan) equipped with an energy dispersive x-ray spectrometer to characterize the morphologies of the products and composition. The transmission electron microscopy studies were carried out on a FEI Tecnai G^2 F20 apparatus with an accelerating voltage of 200 kV. The hydrodynamic diameter and grain size distribution were recorded on a Britain Malvin particle analyzer ZS90. N_2 adsorption-desorption was measured using a Quantachromes NOVA-2100e. The nitrogen adsorption and desorption isotherms were obtained at 77.3 K. The Brunauer-Emmett-Teller (BET) surface area was calculated from the Multi-Point BET Plot.

3. Results and Discussion

3.1. Structural and Compositional Analysis

The crystallinity and phase of the as-obtained products were characterized by X-ray diffraction. The XRD pattern of NiCoP precursor was given in Fig.1a, all of the diffraction peaks can be readily indexed to the hexagonal structure NiCoP with the lattice constant of a=b=5.843 Å, c=3.351 Å, which was nearly consistent with the literature data (JCPDS card No. 71-2336). The diffraction peaks were correspond with the planes of (111), (201), (210), (300), (211), (212), and (222) of NiCoP. However, the XRD pattern of NiCoP/ZnO composites comprised of two sets of diffraction peaks, hexagonal structure NiCoP and hexagonal wurtzite ZnO (JCPDS card No. 36-1451), indicating that NiCoP/ZnO composites have been successfully prepared. The main diffraction peaks were consistent with the planes of (100), (002), (101), (102), (110), and (103) of ZnO. No characteristic diffraction peaks from other phases or impurities were detected, which revealed the high purity of the NiCoP/ZnO composites. Fig.1b showed the (EDS) pattern of the as-prepared NiCoP/ZnO composites. It can be seen that only the peaks for P, Ni, Co, Zn, O, C and Al were appeared. Small peaks of C element came from

the conducting resin and the aluminum peak can be traced to the sample stage. In addition, according to the calculation of peaks area, the molar ratio of NiCoP and ZnO was about 3:1 in the synthesis. It further proved that NiCoP/ZnO were obtained (see the Figure.1).

3.2. Morphology Analysis

The morphology and size of the as-obtained NiCoP and flower-like NiCoP/ZnO microstructure were first confirmed by FE-SEM (shown in Fig.2). Fig.2a showed that the NiCoP samples were composed of uniform microspheres and their average size was 1-2 μm. A close observation by high-magnification SEM image (Fig. 2b) revealed that some smaller nanoparticles could be also observed on the surface of the spheres, indicating that the NiCoP were aggregated by these small nanoparticles. The SEM images of the composites were presented in Fig.2c and 2d. It was clearly seen that ZnO nanosheets were coated on the surface of NiCoP microstructure (shown in Fig.2c). The morphology of the sample average diameter still was in the range of 1-2 μm after ZnO nanosheets were assembled on the surface of NiCoP spheres. However, the diameter of the NiCoP microspheres will increase. Fig.2d was a high-magnification SEM image of flower-like NiCoP/ZnO. It can be observed that the standing nanosheets were cross-linking together on the surface of NiCoP. The nanosheets were about 200-500nm wide and 50nm in thickness. This result was in keeping with the XRD, indicating that the ZnO nanosheets have been successfully assembled on the surface of the NiCoP microspheres (see the Figure.2).

Further detailed structural characterization of the NiCoP and NiCoP/ZnO was performed using transmission electron microscopy (TEM) combined with high resolution transmission electron microscopy (HRTEM). For TEM analysis the structures were ultrasonically dispersed in anhydrous ethanol for 30 min. Fig.3 showed TEM and HRTEM images of the as-prepared NiCoP and flower-like NiCoP/ZnO microstructure. As can be seen from Fig.3a, the NiCoP microspheres had a diameter of was about 2μm and rough edges, which corresponded with the SEM image (Fig.2b). High resolution TEM was carried out to further examine the NiCoP (Fig. 3b). It showed

that the lattice spacing was 0.1101nm and the distance was consistent with the (222) plane of the NiCoP structures. As indicated by Fig. 3c, ZnO nanosheets were assembled on the surface of NiCoP microspheres and the length of the single ZnO nanosheet was about 200nm, which was well matched with the SEM image (Fig.2d). Fig.3d showed the expanded image of the regions A in Fig.3c. It can be seen that the lattice spacing was 0.2481nm and this distance was consistent with the (101) plane of the ZnO structure (see the Figure.3). Besides, the hydrodynamic diameter and grain size distribution of the as-obtained NiCoP and flower-like NiCoP/ZnO microstructure were measured. The samples (NiCoP and NiCoP/ZnO composites) hydrodynamic diameter were 1.318 μm and 1.524 μm, respectively (shown in Fig.4). Fig.4a showed that the NiCoP samples size distribution was about 1μm. The composites size distribution was in the range of 0.8-1.1 μm after ZnO nanosheets were assembled on the surface of NiCoP spheres (Fig.4b). The results were well matched with the SEM and TEM image (see the Figure.4).

3.3. Growth mechanism for the flower-like NiCoP/ZnO

In first step, nickel ions reacted with PH_3 and generated nickel phosphide (shown in Equation (3)). Then the cobalt ions replaced the nickel site in nickel phosphide and further produced NiCoP nuclei. [23] The NiCoP nuclei aggregated and self-assembled to NiCoP spheres due to high surface energy. And in next step, OH^- ions and Zn^{2+} ions combined into the $Zn(OH)_2$ nuclei (shown in Equation (5)). With the time prolonged, the ZnO nanosheets were formed. [24] According to the growth mechanism of ZnO nanosheets, it would grow along the c-axis direction and {0001} plane. So the growth in one more direction lead to the formation of sheet-like structures. [25] Finally ZnO nanosheets were assembled on the surface of the as-prepared NiCoP microspheres. [26] The whole growth process of the flower-like NiCoP/ZnO was described in Scheme 1 (see the Scheme 1).

$$P_4+HOCH_2CH_2OH \rightarrow PH_3+H_3PO_3+CH_3CHO \quad (1)$$

$$H_3PO_3 \rightarrow PH_3+H_3PO_4 \quad (2)$$

$$9PH_3+16NiCl_2 \rightarrow 8Ni_2P+27HCl\uparrow+PCl_5 \quad (3)$$

$$9PH_3+16CoCl_2+8Ni_2P \rightarrow 16NiCoP+27HCl\uparrow+PCl_5 \quad (4)$$

$$Zn^{2+}+2OH^- \rightarrow Zn(OH)_2 \quad (5)$$

$$Zn(OH)_2 \rightarrow ZnO+H_2O \quad (6)$$

3.3. Adsorption performances of NiCoP and NiCoP/ZnO

To evaluate the adsorption performances of the samples, the adsorption experiments of some organic dyes (Congo red and Malachite green) were carried out and the experimental results were shown in Fig.6. It showed the UV-vis adsorption spectra of the Congo red and Malachite green solution. It can be observed that the as-prepared samples (NiCoP and NiCoP/ZnO composites) owned different adsorption activity for different organic dyes. It was found that the adsorption ratios of two dyes (Congo red and Malachite green) were reached to 40.23% and 72.34% in the presence of NiCoP, respectively. The adsorption ratios of two dyes (Congo red and Malachite green) were 64.52% and 86.78% in the presence of NiCoP/ZnO (see the Figure.6). As a whole, compared to the NiCoP, when ZnO nanosheets were assembled on the surface of NiCoP, the adsorption activity was improved. The enhanced adsorption activity may be due to the assembling of ZnO nanosheets onto the surface of NiCoP spheres modifies the surface state of materials. It is known that size and surface areas have an important effect on the adsorption activity, so the surface areas of the as-obtained samples were measured. The Nitrogen adsorption-desorption isotherm curves of the samples were shown in Fig. 5. It can be seen from Fig. 5a and 5b that the Nitrogen adsorption-desorption isotherm curves belong to type IV isotherm, and the hysteresis loop belong to type H1. [27] The BET surface area for the as-obtained samples calculated from the linear part of the BET plot are about 24.450 $m^2 g^{-1}$ (Fig. 5a) and 88.412 $m^2 g^{-1}$ (Fig. 5b).The reason is that nanoscale oxidized Zn particles have quantum dimension effect and larger surface area, which not only can provide the larger contact area between samples and dye molecule but also can offer more surface sites for the generation of free radicals.

In addition, the surface active sites which derive from the different of surface bonding and particles inner structures is conducive to form the uneven atomic steps. [28] Those will accelerate the adsorption of dyes. The surface state of the samples is another key factor which impact the adsorption activity. It is commonly believed that the dyes with anionic or cationic groups can absorb on the surface of the samples with contrary charges via electrostatic interaction, [29] which further promote the adsorption process of dyes. Based on this conjecture, the Zeta potential of the samples were detected. As shown in the of Fig.7a and 7b, all the samples of NiCoP and NiCoP/ZnO exhibited the negative charge, and it can facilely adsorb the dyes with cationic groups such as Malachite green (see the Figure.7).

4. Conclusion

In this paper, flower-like NiCoP/ZnO composites were successfully synthesized via a simple solvothermal route at 120 ℃ for 10 h. The characterization results of XRD, SEM, TEM showed that the as-prepared products were composed of the NiCoP hexagonal and ZnO hexagonal wurtzite structure. It was found that the ZnO nanosheets which have the wide of 200-500nm and the thickness of 50nm were coated on the surface of the obtained NiCoP microspheres with the average diameter of 1-2 μm. For the absorption performance, the BET area and zeta potential were measured. The large surface area and electrostatic interaction were conducive to promote the adsorption of dyes. Furthermore, the adsorption experiments indicated that the composites adsorption ratios of two dyes (Congo red and Malachite green) were increased to 64.52% and 86.78% compared with NiCoP monomer. Superior adsorption performance may find its potential application in wastewater treatment.

Acknowledgements

The authors appreciate the financial support from the National Natural Science Foundation of China (21301113), the Scientific Research Planning Program of the Education Department of Shaanxi Province

(2013JK0684), and the Graduate Innovation Fund of Shaanxi University of Science and Technology.

References

[1] V.R. Stamenkovic, B. Fowler, B.S. Mun, G. Wang, P.N. Ross,C.A. Lucas, and N.M. Markovic, J. Science., 2007, **315**, 493-497.

[2] B. Lim, M. Jiang, P.H.C. Camargo, E.C. Cho, J. Tao, X. Lu, Y. Zhu, and Y. Xia, J. Science., 2009, **324**, 1302-1305.

[3] T. Omori, K. Ando, M. Okano, X. Xu, Y. Tanaka, I. Ohnuma, R. Kainuma, and K. Ishida, J. Science., 2011 **333**, 68-71.

[4] E. González, J. Arbiol, and V. F. Puntes, J. Science., 2011, **334**, 1377-1380 .

[5] J. W. Hong, D. Kim, Y. W. Lee, M. Kim, S.W. Kang, and S. W. Han. J. Small., 2013, **9**, 660-665.

[6] S. Habas, H. Lee, V. Radmilovic, G. A. Somorjai, and P. Yang, Nat. Mater., 2007, **6**, 692-697.

[7] Y. Yu, Q. Zhang, B. Liu, J. Y. Lee, and J. Am, J. Chem. Soc., 2010, **132**, 18258-18265.

[8] J. Wu, P. Li, and H. Yang, Chem Soc Rev., 2012, **41**, 8066-8074.

[9] J. B. Tong, Y. Y. Liu, and S. L. Liu, J. Synth. Cryst., 2015, 1, 030.

[10] B. Liu, J. Xu, S. H. Ran, Z. R. Wang, D. Chen, and G. Z. Shen, Cryst Eng Comm., 2012, **14**, 4582-4588.

[11] J. Tian, Y. H. Sang, G. W. Yu, H. D. Jiang, X. N. Mu, and H. Liu, Adv. Mater., 2013, **25**, 5074.

[12] W. N. Jia, X. Wu, B. X. Jia, F. Y. Qu, and H. J. Fan, Sci. Adv. Mater., 2013, **5**, 1329-1336.

[13] H. B. Zeng, G. T. Duan, Y. Li, S. K. Yang, X. X. Xu, and W. P. Cai, Adv. Funct. Mater., 2010, **20**, 561-572.

[14] Q. X. Wang, L. P. You, X. Z. Zhang, M. Wang, Y. Z. Lv, and L. Gu, J. Rare Metals., 2006, **25**, 193-199.

[15] V. V. Pokropivny, and M. M. Kasumov, J. Tech Phys Lett., 2007, **33**, 44-47.

[16] X. H. Xie, X. J. Li, and H. H. Yan, J. Mater Lett., 2006, **60**, 3149-3152.

[17] A. D Lazareck, S. G Cloutier, T .F Kuo, B. J Taft, S. O Kelley, and J. M Xu, J. Nanotechnology., 2006, **17**,

2661-2664.

[18] H. Q. Wang, G. H. Li, L. C. Jia, G. Z. Wang, and C. J. Tang, J. Phys Chem C., 2008, **112**, 11738−11743.

[19] T. M. Shang, J. H Sun, Q. F. Zhou, and M. Y. Guan, J. Cyst Res Technol., 2007, **42**, 1002-1006.

[20] Z. Y. Fan, D. W. Wang, P. C. Chang, W. Y. T Seng, and J.G. Lu, Appl. Phys. Lett., 2004, **85**, 5923-5925.

[21] A. Wei, L. Xiong, L. Sun, Y. J. Liu, W. W. Li, W. Y. Lai, X. M. Liu, L. H. Wang, W. Huang, and X. C. Dong, Mater. Res. Bull., 2013, **48**, 2855-2860.

[22] Y. H. Chen, Y. F. Zheng, X. G. Zhang, Y. F. Sun, and Y. Z. Dong, China Sci Series G., 2005, **48**, 188-200.

[23] S Zhang, L Song, and Q Wu, Ceram. Int., 2014, **40,** 5339-5342.

[24] F Yan, S W Zhang, Y Liu, H F Liu, F Y Qu, X Cai, and X W, Mater. Res. Bull., 2014, **59,** 98-103.

[25] Ahmad Umar, and Y B Hahn, Nanotech., 2006, **17,** 2174-2180.

[26] S L Liu, H L Li, and L Yan, Mater. Res. Bull., 2013, **48**, 3328-3334.

[27] W. Wang, K. Zhang, Y. Yang, H Liu, Z Qiao, and H Luo, Micropor. Mesopor. Mat., 2014, **193,** 47-53.

[28] R. Q. Gan, D. D. Huang, and Z. K .Wang, Adv. Mater. Res., 2013, **734**, 2338-2341.

[29] I. K. Konstantinou, and T. A. Albanis, Appl. Catal. B., 2004, **49**, 1-14.

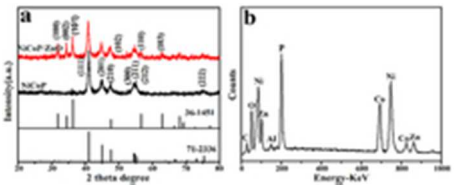

Fig. 1 (a) The XRD pattern of the NiCoP and NiCoP/ZnO; (b) EDS spectrum of the as-prepared NiCoP/ZnO.
19x7mm (300 x 300 DPI)

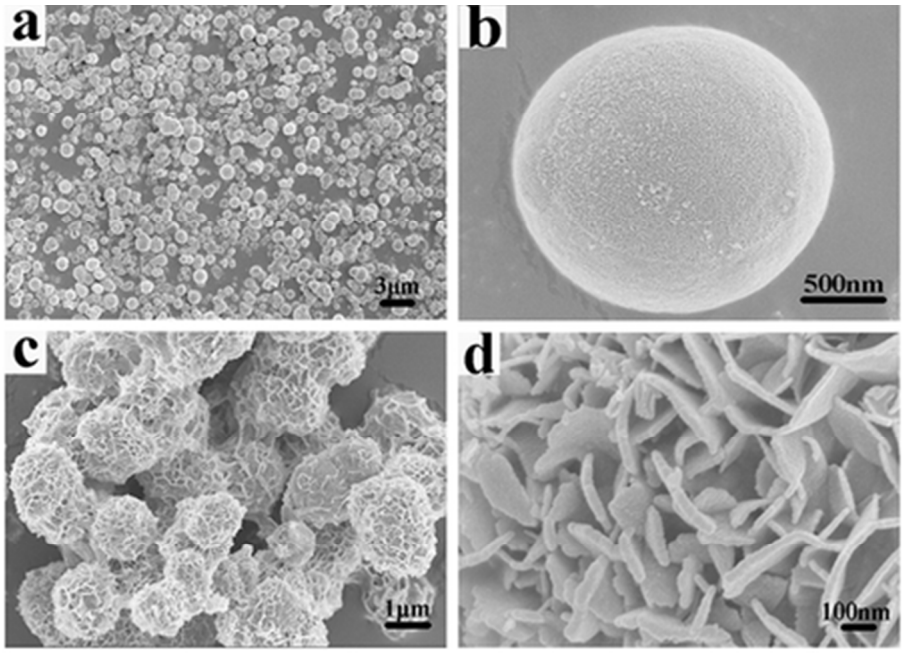

Fig. 2 The SEM images of the as-prepared NiCoP (a and b) and flower-like NiCoP/ZnO microstructure(c and d).
38x27mm (300 x 300 DPI)

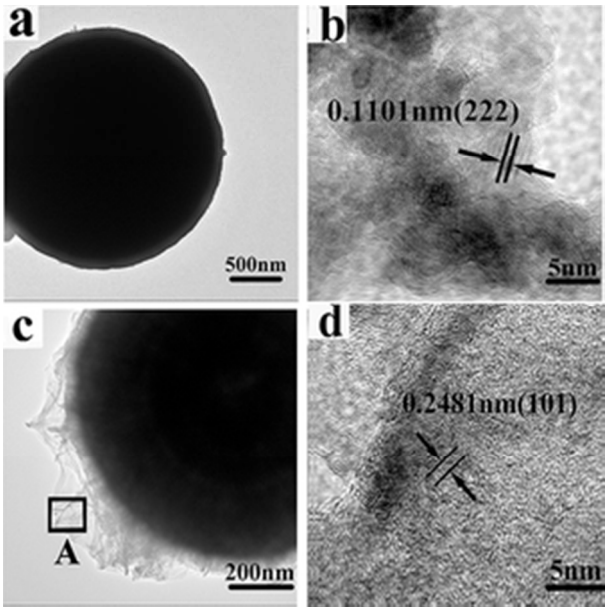

Fig. 3 (a) TEM image of the NiCoP; (b) HRTEM image the NiCoP; (c) TEM image of the NiCoP/ZnO; (d) HRTEM image of region A.
25x25mm (300 x 300 DPI)

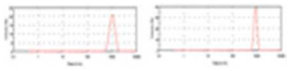

Fig. 4 The grain size distribution of the samples: (a) NiCoP; (b) NiCoP/ZnO.
11x2mm (300 x 300 DPI)

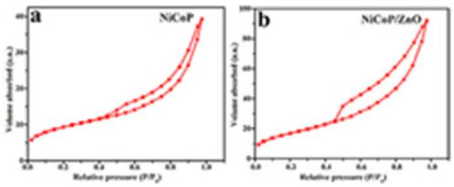

Fig. 5 Nitrogen adsorption-desorption isotherm curves of the samples: (a) NiCoP; (b) NiCoP/ZnO.
19x7mm (300 x 300 DPI)

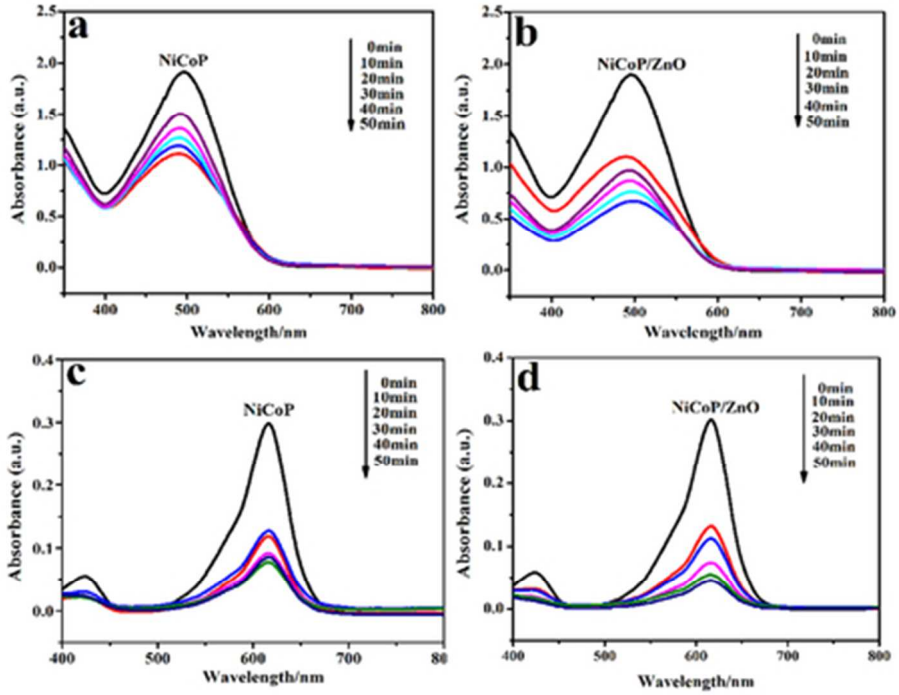

Fig. 6 UV-vis adsorption spectra of the different dyes (a-b)Congo red; (c-d) Malachite green.
38x29mm (300 x 300 DPI)

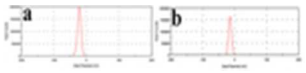

Fig. 7 Zeta potential of the samples: (a) NiCoP; (b) NiCoP/ZnO.
12x2mm (300 x 300 DPI)

Scheme 1 Schematic illustration of growth mechanism of flower-like.
9x1mm (300 x 300 DPI)